A new method for identifying diagnostic rich frequency bands under varying operating conditions

Stephan Schmidt[1] Alex R. Mauricio[2] P. Stephan Heyns[3] Konstantinos C. Gryllias[4]

[1]Centre for Asset Integrity Management, University of Pretoria, Pretoria, South Africa
stephan.schmidt@up.ac.za

[2]Department of Mechanical Engineering, PMA Division, KU Leuven, Leuven, Belgium
Dynamics of Mechanical and Mechatronic Systems, Flanders Make, Belgium
alex.ricardomauricio@kuleuven.be

[3]Centre for Asset Integrity Management, University of Pretoria, Pretoria, South Africa
stephan.heyns@up.ac.za

[4]Department of Mechanical Engineering, PMA Division, KU Leuven, Leuven, Belgium
Dynamics of Mechanical and Mechatronic Systems, Flanders Make, Belgium
konstantinos.gryllias@kuleuven.be

Abstract

Performing condition monitoring under time-varying operating conditions is challenging. The varying operating conditions impede the ability of conventional fault diagnosis methods to detect damage on rotating machine components such as bearings and gears. This paper investigates a new method for identifying diagnostic rich frequency bands under time-varying operating conditions. This method uses the order-frequency spectral coherence and a feature, which is dependent on the cyclic order of interest and the frequency resolution of the spectral coherence, to decompose the signal into a feature plane. Thereafter, the spectral frequency and the spectral frequency resolution that maximise the feature plane are used to design a bandpass filter. The bandpass filter extracts a diagnostic rich signal, which can be analysed by using the squared envelope spectrum or the synchronous average. The proposed method is compared to the fast kurtogram on a numerical gearbox dataset as well as on an experimental gearbox dataset, with very promising results obtained.

1 Introduction

Effective fault diagnosis techniques are important for expensive assets such as wind turbines, because this can result in early detection of faults, their characteristics can easily be understood (e.g., which component is damaged) and subtle changes in the damage (i.e. deterioration) can be monitored. Many rotating machines inherently operate under time-varying operating conditions, which impede effective fault diagnosis. Hence, it is important to use condition monitoring techniques that are able to diagnose damaged machine components under time-varying operating conditions.

Damaged rotating machine components such as bearings result in periodical excitations of the structure at a rate dependent on the kinematic characteristics of the component (e.g. ball pass order of the outer race, shaft rotation). This angle-dependent periodical excitation of the time-invariant structure generates signals that can be approximated as angle-time cyclostationary [1]. Abboud et al. [1, 2, 3] extended the suite of conventional time and angle cyclostationary techniques to time-varying speed conditions with tools such as the Order-Frequency Spectral Coherence (OFSCoh) being one of the most powerful fault diagnosis techniques for bearings under varying speed conditions.

However, in condition monitoring it is usually desired to utilise simple metrics or representations for making decisions (e.g. a spectrum is preferred instead of a time-frequency spectrum). Hence, the enhanced envelope spectrum and the even more powerful Improved Envelope Spectrum (IES), both calculated from the spectral coherence or the spectral corelation, can be used to diagnose the machine. For the IES, it is very important to select carefully the integration band to ensure that the IES has an optimal signal-to-noise ratio. This means that it is important to be able to identify frequency bands that are rich with diagnostic information. Identifying diagnostic rich frequency bands is also important for calculating the synchronous average and the squared envelope spectrum [4].

The spectral kurtosis and the related kurtogram are effective for identifying frequency bands with much impulsive information [5, 6]. This is very appropriate for diagnostics, because bearing damage [4, 5] and gear damage [7] result in vibration signals containing bandlimited impulses. However, the kurtogram is sensitive to transients not related to the condition of the machine and it is not possible to investigate the optimal frequency band to detect damage associated with a specific cyclic order. Recently, new methods such as the infogram [8] and the IESFOgram [9] have been proposed for identifying frequency bands that are rich with diagnostic information by improving the shortcomings of the kurtogram.

A new method is investigated in this paper that is able to identify a frequency band that contains diagnostic information related to a specific machine component under time-varying operating conditions. This has a significant advantage over conventional methods, because incipient damage components that are normally masked by other dominant signal components and distorted by time-varying operating conditions, can be extracted from the signal and used to diagnose the machine. The performance of this method is compared to the Fast Kurtogram on numerical gearbox data as well as on experimental gearbox data, both acquired under time-varying operating conditions.

The outline of this paper is as follows: In Section 2, the proposed method is presented, whereafter it is investigated on phenomenological gearbox data in Section 3 and experimental gearbox data in Section 4. In the last section, Section 5, some conclusions are extracted and some recommendations are made for future investigations.

2 Methodology

2.1 Overview of the methodology

An overview of the methodology is presented in Figure 1. The measured vibration signal and the corresponding rotational speed (or phase) is given as inputs, whereafter an Order-Frequency Spectral Coherence (OFSCoh) is calculated for a specific window length. A feature is extracted from each frequency band of the calculated OFSCoh. This process is repeated for the set of window lengths under consideration, whereafter a feature plane is constructed. The feature plane contains the value of the feature for different combinations of centre frequencies and window lengths (or frequency resolutions). Thereafter, the feature plane is maximized to obtain the parameters of a bandpass filter. This bandpass filter is used to extract a signal that is rich with diagnostic information from the original signal, whereafter the filtered signal can be analysed to infer the condition of the machine component.

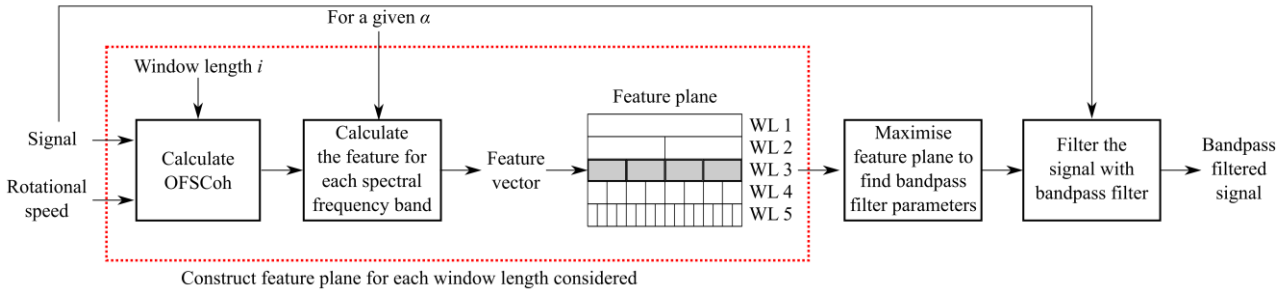

Figure 1: The proposed method for identifying frequency bands that are rich with diagnostic information.

The subsequent sections give detailed information on each step in the proposed method.

2.2 Order-Frequency Spectral Coherence (OFSCoh)

The impulses generated by components such as bearings are periodic in the angle domain, while they manifest in the time-invariant frequency bands. This means that the OFSCoh can be used to identify the resonance bands that are excited at specific cyclic orders. The OFSCoh [2]

$$\gamma_{xx}(\alpha, f) = \frac{S_{xx}(\alpha, f)}{\left(S_{xx}(0, f) S_{x_\alpha x_\alpha}(0, f)\right)^{1/2}} \tag{1}$$

provides a two-dimensional view of the modulating frequencies (i.e. cyclic orders) and their carriers (i.e. spectral frequencies) in the signal *x(t)*. The Order-Frequency Spectral Correlation (OFSC) [2]

$$S_{xx}(\alpha, f) = \lim_{W \to \infty} \frac{1}{\Phi(W)} E\left\{F_W\left(x(t)\right)^* F_W\left(x(t) e^{-j\alpha\theta(t)} \dot{\theta}(t)\right)\right\} \tag{2}$$

is used to calculate the OFSCoh in Equation (1). The expectation operator is denoted E, the Fourier transform is denoted F_w and $\Phi(W)$ denotes the phase of the shaft during the measurement time period W. The instantaneous phase of the shaft is denoted θ. It is easier to detect non-dominant components by using the OFSCoh as opposed to the OFSC.

Estimators need to be used to calculate the OFSCoh for the measured data, with the Welch estimator as proposed in Ref. [2], used in this work. The Welch estimate of the OFSCoh is denoted $\gamma_{xx}(\alpha, f; \Delta f)$, where Δf is the frequency resolution that is used to obtain the estimate.

2.3 Frequency Band Identification (FBI)

It is possible to use a one-dimensional metric such as the kurtosis to identify the frequency band of interest. However, one-dimensional metrics do not allow different signal components to be distinguished from one another, which may result in a frequency band to be identified that is not necessarily of interest. Hence, a more advanced metric is required.

2.3.1 Feature extraction

Ref. [4] uses a metric to quantify the quality of the Squared Envelope Spectrum (SES). If their metric is large, it means that the diagnostic information is dominant with respect to the noise level in the SES, while a small metric indicates that it could be difficult to detect the cyclic components in the SES. The authors estimated the noise level with the median because the median is robust to outliers generated by the cyclic components in the SES.

We used this metric as inspiration for designing the feature to identify the frequency band of interest, with the following feature obtained for the cyclic order set $\{\alpha_f\}$:

$$\Psi_{xx}(f, \Delta f; \{\alpha_f\}) = \sum_{\{\alpha_f\}} \frac{|\gamma_{xx}(\alpha_f, f; \Delta f)|^2}{median\left(|\gamma_{xx}(\alpha_f, f; \Delta f)|^2\right)} \tag{3}$$

The numerator contains the squared magnitude of the spectral coherence for a specific window length Δf. The denominator contains the median function, which is calculated for the squared magnitude of the spectral coherence and is used to estimate the noise level in the OFSCoh. The following points are important considerations when calculating the feature for practical signals:

1. The analytical cyclic orders may be different from the actual cyclic orders due to slip and therefore the maximum of a range of $[0.9\alpha_f, 1.1\ \alpha_f]$ is calculated to estimate the numerator.
2. The median of the squared magnitude OFSCoh cannot be calculated at $\alpha=\alpha_f$ and therefore it needs to be estimated from the discrete OFSCoh data. Hence, the median of the squared magnitude of the OFSCoh in the range of $[\alpha_f - 1, \alpha_f + 1]$ is used to estimate the denominator.

This feature also has similarities to the feature used by the IESFOgram [9]. In the latter method the ratio of the signal components in the IES are calculated with respect to the mean of the IES in the predefined bandwidth.

2.3.2 Feature plane construction and maximisation

The feature is calculated for each frequency band in the OFSCoh. The Welch estimator of the OFSCoh depends on a number of parameters, namely, the window length, the window overlap as well as the number of points used to calculate the FFT. It is best to use an overlap longer than 75% of the window length, however, the window length needs to be determined prior to the analysis. It is also necessary to estimate the frequency bandwidth and not only the centre frequency for designing the bandpass filter parameters. Hence, the following procedure is used to simultaneously optimise the centre frequency and frequency bandwidth of the frequency band of interest: Firstly, the OFSCoh is calculated for a specific window length, whereafter the feature is calculated for each spectral frequency band in the OFSCoh. This process is repeated for each window length under consideration, whereafter the feature plane is obtained. The frequency band parameters are identified by finding the centre frequency and frequency bandwidth that maximise the feature plane. This is a very similar procedure to the kurtogram and the infogram, but instead of using the short-time Fourier transform, the OFSCoh is used, and instead of maximising a scalar value (e.g. spectral kurtosis), the maximisation is done for a set of cyclic orders. This allows the optimal frequency band to be determined to detect a set of cyclic orders.

The identified frequency band parameters can be used to calculate the IES or to extract a bandlimited signal. In this work, we used the frequency band parameters to design a bandpass filter, whereafter the bandpass filtered signal is interrogated. The bandpass filtered signal can subsequently be analysed with techniques such as the Synchronous Average (SA) [10] and the Squared Envelope Spectrum (SES) [3].

2.4 Computational aspects

Even though real-time condition monitoring is rarely required in practice, it is still necessary to provide answers in a reasonable time. The Welch-based estimator of the OFSCoh has very good bias and variance properties, but is very expensive to calculate for large datasets, especially for high rotational speed applications. If the cyclic orders of interest are known a priori, it is possible to only estimate the OFSCoh for specific cyclic orders; however, even this may be impractical for complex gearboxes found in wind turbines and helicopters, which may have many cyclic orders of interest. Fortunately, there has been very exciting developments in this field, where fast (and faster) estimators of the spectral correlation are proposed, which could make this method significantly faster to be calculated [11, 12].

3 Numerical gearbox data

In this section, we investigate the method and compare it to the kurtogram on data generated from a phenomenological gearbox model. In the next section, an overview is given of the model and the generated data, whereafter the Fast Kurtogram (FK) is used on the dataset in Section 3.2. The results of the proposed method are presented and discussed in Section 3.3.

3.1 Phenomenological Gearbox Model (PGM)

The Phenomenological Gearbox Model (PGM) proposed in Ref. [3] is used to generate a casing vibration signal. The casing vibration signal

$$x(t) = x_b(t) + x_{rg}(t) + x_n(t) \tag{4}$$

contains a bearing component $x_b(t)$, a random gear component $x_{rg}(t)$ and a broadband noise component $x_n(t)$. The generalised synchronous average can be used to attenuate the deterministic gear components attributed to the meshing of gears as described by Abboud et al. [3] and therefore they are not included in this model. The bearing component is generated by bearing damage on the outer race

$$x_b(t) = M(\omega(t)) \cdot h_b(t) \otimes \sum_{k=1}^{K_b} A_k \cdot \delta(t - T_k) \tag{5}$$

where T_k denotes the time-of-arrival of the kth bearing impulse, which incorporates the varying speed conditions and the slip. The amplitude of the kth impulse, denoted A_k, is sampled from a uniform distribution. The raw bearing impulses are filtered through the structure, which is assumed to have an impulse response

function of a single degree-of-freedom system h_b. The modulating function $M(\omega(t)) = \omega^2$ is used to simulate the varying amplitude induced by time-varying operating conditions and is assumed to be the same for all signal components for the sake of simplicity.

The random gear component

$$x_{rg}(t) = M(\omega(t)) \cdot h_{rg}(t) \otimes \left(\varepsilon(t) \cdot \sum_{k=1}^{Krg} B_k \cdot \sin\left(k \cdot \int_0^t \omega(t)dt + \varphi_k \right) \right) \tag{6}$$

is attributed to gear damage and contains the random variable $\varepsilon(t)$ which is sampled from a zero mean, unit variance normal distribution, and B_k and φ_k are, respectively, the amplitude and the phase of the kth harmonic of the component. There are K_{rg} harmonics in the vibration signal. The noise component

$$x_n(t) = M(\omega(t)) \cdot \varepsilon(t) \tag{7}$$

is generated by a zero mean Gaussian distribution with its amplitude dependent on the rotational speed of the system. The natural frequency of the impulse response function of the bearing and the gear components are 7 kHz and 1.3 kHz respectively. The fundamental cyclic order of the distributed gear damage is 1.0 shaft order, while the fundamental cyclic order of the outer race bearing damage component is 4.12 shaft orders.

A single dataset is investigated in this paper with the time-varying speed profile *ω(t)* and the different signal components shown in Figure 2. This system operates under constant load conditions.

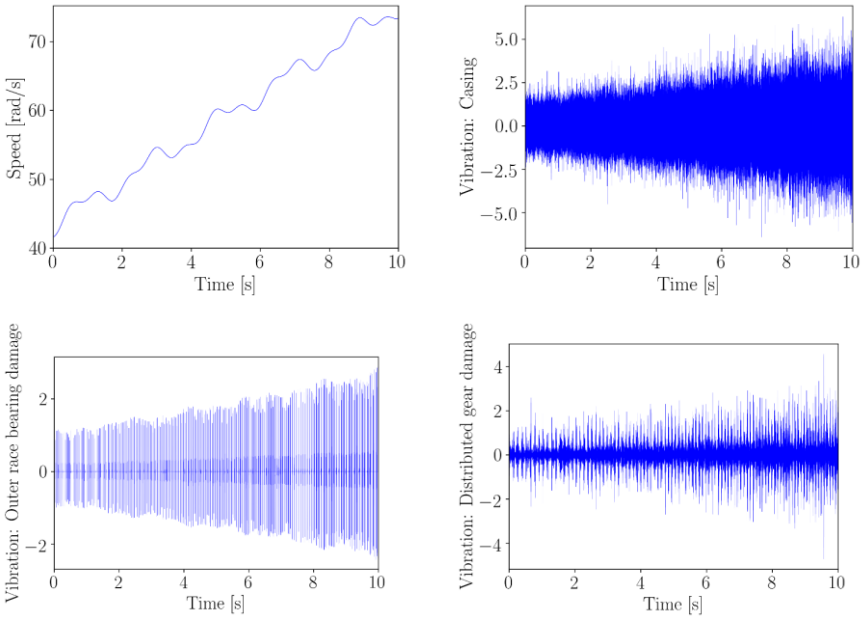

Figure 2: The speed profile, the casing vibration signal and the bearing and random gear components of the phenomenological gearbox model are presented.

The varying speed conditions result in the amplitude and the instantaneous frequency of the signal components to be dependent of time. The relative magnitudes of the components were chosen so that the dominant distributed gear damage component impedes the ability to detect the bearing component. Hence, the focus of the subsequent investigations is to highlight how the proposed method can be used to detect weak components in the presence of dominant components and to show that it is possible to distinguish between the two. In the next section the kurtogram is investigated on the generated dataset.

3.2 Application of the Fast Kurtogram (FK)

The Fast Kurtogram (FK), developed in Ref. [6], is a faster estimator of the kurtogram than the conventional short-time Fourier transform-based estimator and is used in this work. The kurtogram is based on the spectral kurtosis [5], a very useful technique to identify frequency bands that contain transient information (as typically seen by bearing and gear damage). The FK is applied to the casing vibration signal (see Equation (4)) of the PGM with the result shown in Figure 3.

The FK is maximum at a frequency band with a centre frequency of 1328.12 Hz. This is the frequency band associated with the distributed gear damage component. The frequency band of the bearing damage at 7.0 kHz can also be seen in Figure 3; however, its magnitude is significantly smaller than the magnitude of the gear component.

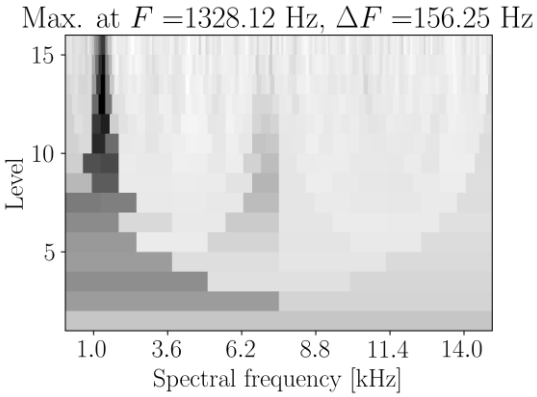

Figure 3: The kurtogram of the PGM's vibration signal.

The implication of this is that without careful consideration, only the dominant impulsive frequency band will be detected by the FK, with a non-dominant frequency band easily missed in the condition interrogation process.

This is corroborated by the results of the Squared Envelope Spectrum (SES) seen in Figure 4. The SES of the raw signal (i.e. without bandpass filtering the signal) and the SES of the filtered signal contains the same information. The fundamental component of the distributed gear damage at one shaft order and its harmonics are clearly seen in both spectra, while the bearing component is not seen.

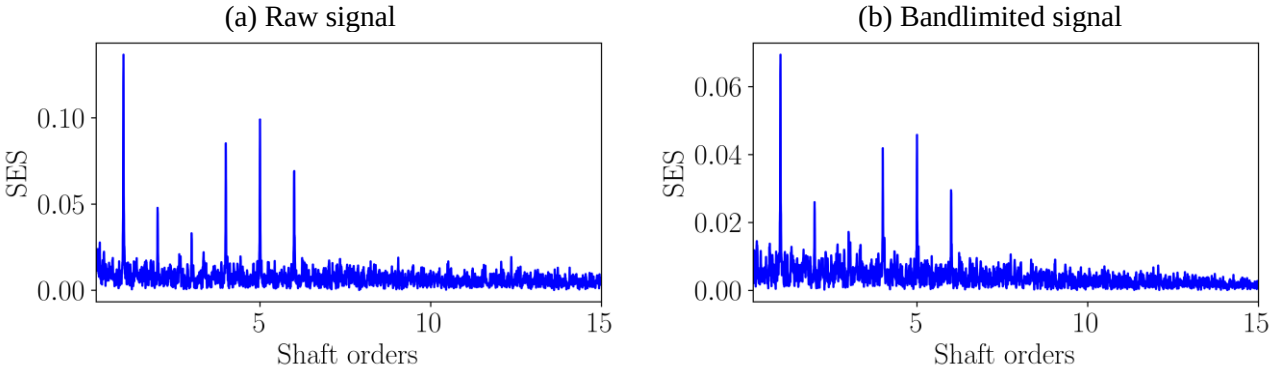

Figure 4: The Squared Envelope Spectrum (SES) of the raw vibration signal and of the bandlimited signal obtained with the Fast Kurtogram (FK) for the PGM.

It is important to emphasise that due to the statistical characteristics of the distributed gear damage component, it is not possible to remove it using cepstrum pre-whitening or the generalised synchronous average [3]. The proposed method is investigated in the next section.

3.3 Application of the proposed method

The proposed method is applied with the procedure discussed in Section 2, with the bearing and gear being monitored for damage. Therefore, the feature, calculated with Equation (3), is calculated for the gear with $\{\alpha_f\}=\{1.0, 2.0, 3.0\}$ (denoted α=1.0 in the figures) and for the bearing with $\{\alpha_f\}=\{4.12, 8.24, 12.36\}$ (denoted α=4.12 in the figures), which result in two feature planes that are maximised independently. The feature plane of the gear and the bearing are shown in Figure 5(a) and Figure 5(b) respectively.

It is evident that the feature plane is clearly very dependent on the cyclic order that is used. Large values are obtained in Figure 5(a) in the region of 1.3 kHz, while large values are obtained in Figure 5(b) in the

region of 7 kHz. The optimal value for the gear in Figure 5(b) differs slightly from the analytical value, because the gear component is very dominant, which results in the different blocks to have features with very similar values, i.e. any of the blocks, could be used for detecting the gear.

The SES of the raw and bandlimited signals of the two signal components are shown in Figure 6. The SES of the bandlimited gear signal, presented in Figure 6(b), does not improve the SES of the raw signal, presented in Figure 6(a), because the gear component is already very dominant in the SES.

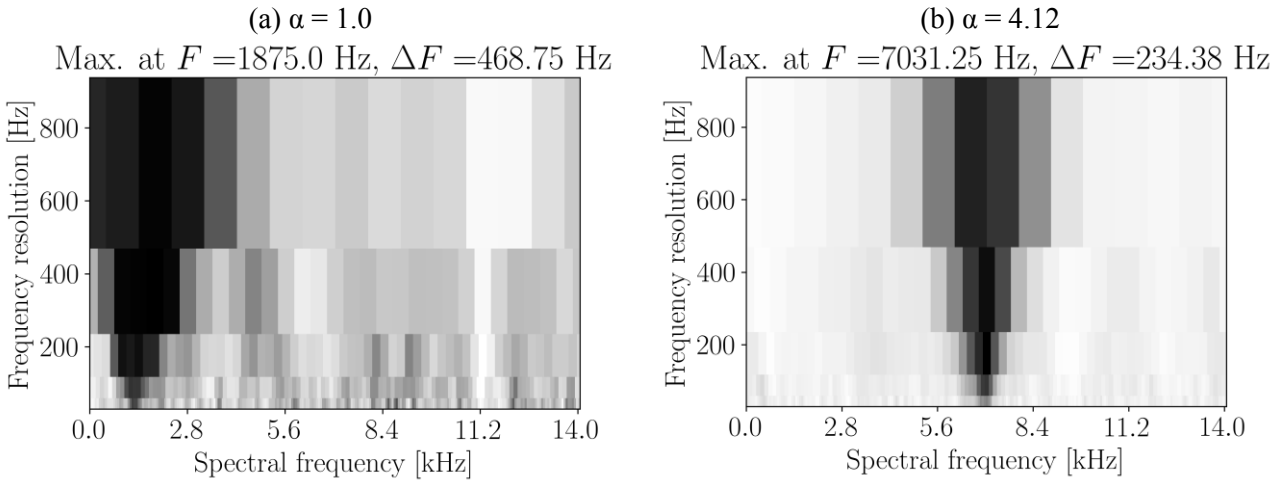

Figure 5: The feature plane obtained with the proposed method for the gear component (a) and the outer race bearing component (b) of the PGM. The colour scales are not the same in the two plots.

A significant improvement can be seen for the SES of the bearing component. The bearing component cannot be detected in Figure 6(c), but after identifying the appropriate frequency band with the proposed method, it is possible to obtain a SES that clearly highlights the damaged bearing component as seen in Figure 6(d).

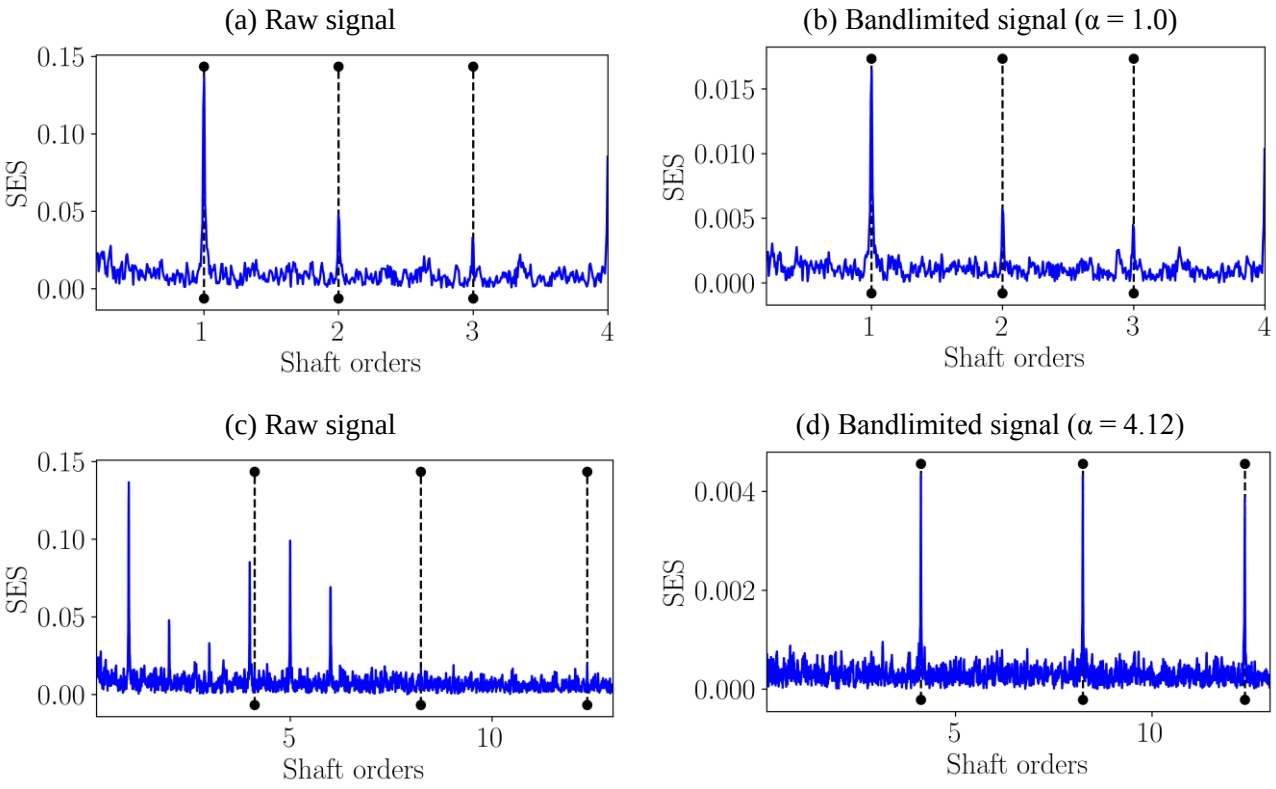

Figure 6: The Squared Envelope Spectra (SES) of the raw and bandlimited signals are shown for the gear component in (a) and (b) and for the outer race bearing component in (c) and (d) for the PGM.

This highlights the benefit of using the proposed method; if the signal component is dominant in the spectrum then the kurtogram can lead to similar results (as seen when comparing the results in Figure 4(b) and Figure 6(b)). However, the proposed method has sufficient flexibility to identify frequency bands for signals with low signal-to-noise ratios as well.

4 Experimental investigation

In this section, the proposed method is investigated on an experimental dataset. A brief overview of the experimental data is given in Section 4.1, whereafter the FK is applied to the dataset in Section 4.2 and the proposed method is investigated in Section 4.3.

4.1 Overview of the experimental dataset

The method is applied and verified in this section on an experimental gearbox dataset that has been acquired in the Centre for Asset Integrity Management (C-AIM) laboratory at the University of Pretoria. The experimental setup contains three helical gearboxes, an alternator and an electrical motor. The alternator and the electrical motor were used to induce the time-varying speed and load conditions shown in Figure 7 on the monitored gearbox. One of the helical gearboxes was damaged with the damaged gear shown in Figure 8(a) and operated for approximately 20 days whereafter the tooth failed as shown in Figure 8(b). A vibration and a tachometer measurement, taken after approximately five days of testing, are used in this paper. The gear rotates at 1.0 shaft order, while the pinion rotates at 1.85 shaft order. More information on the experimental setup can be found in Ref. [13].

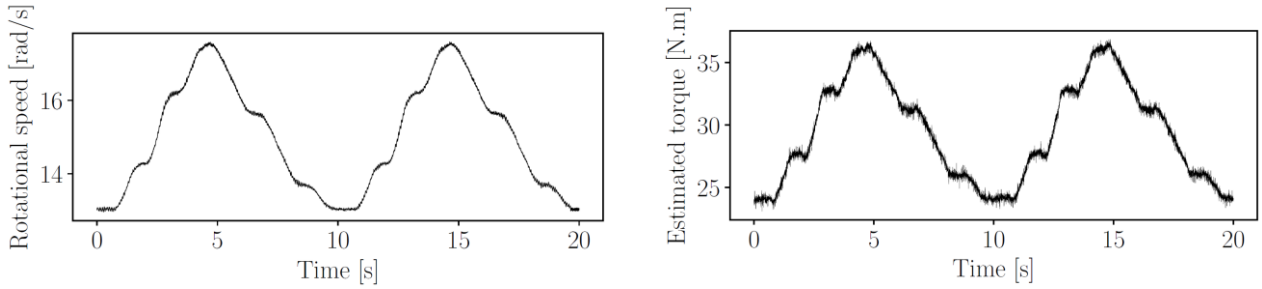

Figure 7: The operating conditions during the measurement period.

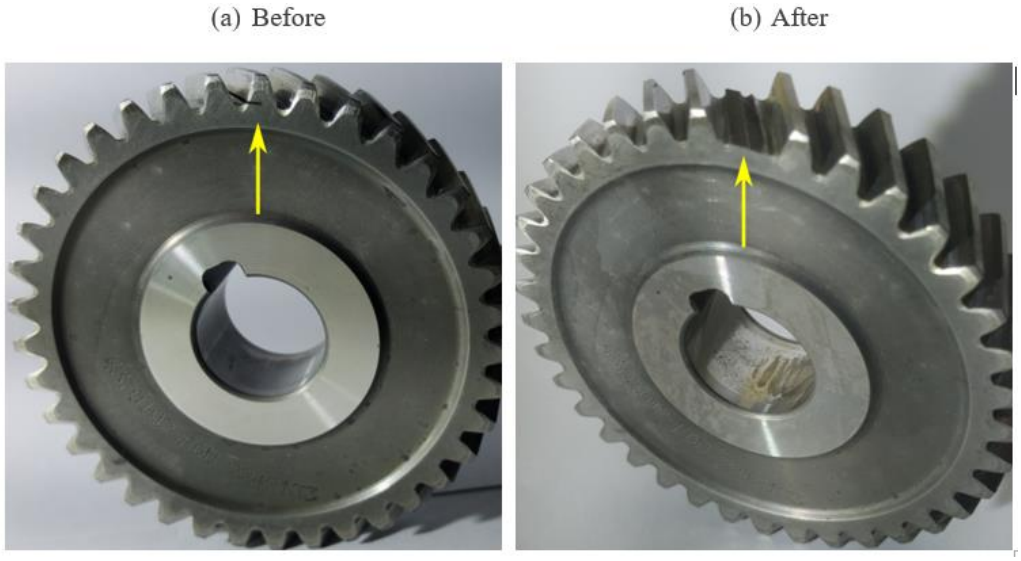

Figure 8: The gear of the helical gearbox with the seeded fault before the fatigue experiment (a) and after the fatigue experiment was completed (b).

4.2 Application of the Fast Kurtogram (FK)

The FK is applied on the dataset with the decomposition shown in Figure 9. Very large values are seen in the higher frequency bands. This is attributed to the presence of bandlimited transients that manifest at the frequency band 8-12 kHz at a cyclic order of approximately 5.5 shaft orders.

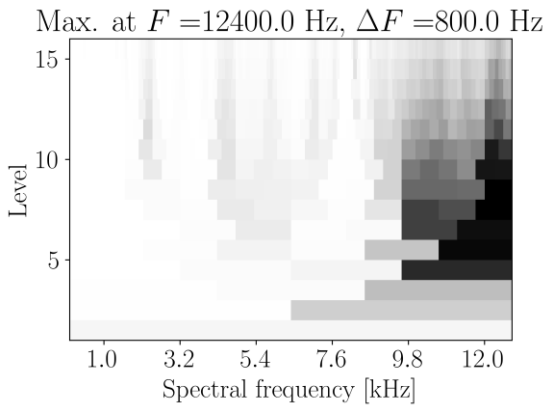

Figure 9: The kurtogram of the experimental gearbox dataset.

The SA is used to interrogate the presence of damage on the gear in Figure 10. The SA of the raw and the bandlimited signals are shown in Figure 10(a) and (b). It is not clear from the raw signal in Figure 10(a) what the condition of the gear is, but the transients that are retained by the bandpass filtering process dominate the synchronous average and make it especially difficult to infer the condition of the machine from the result in Figure 10(b).

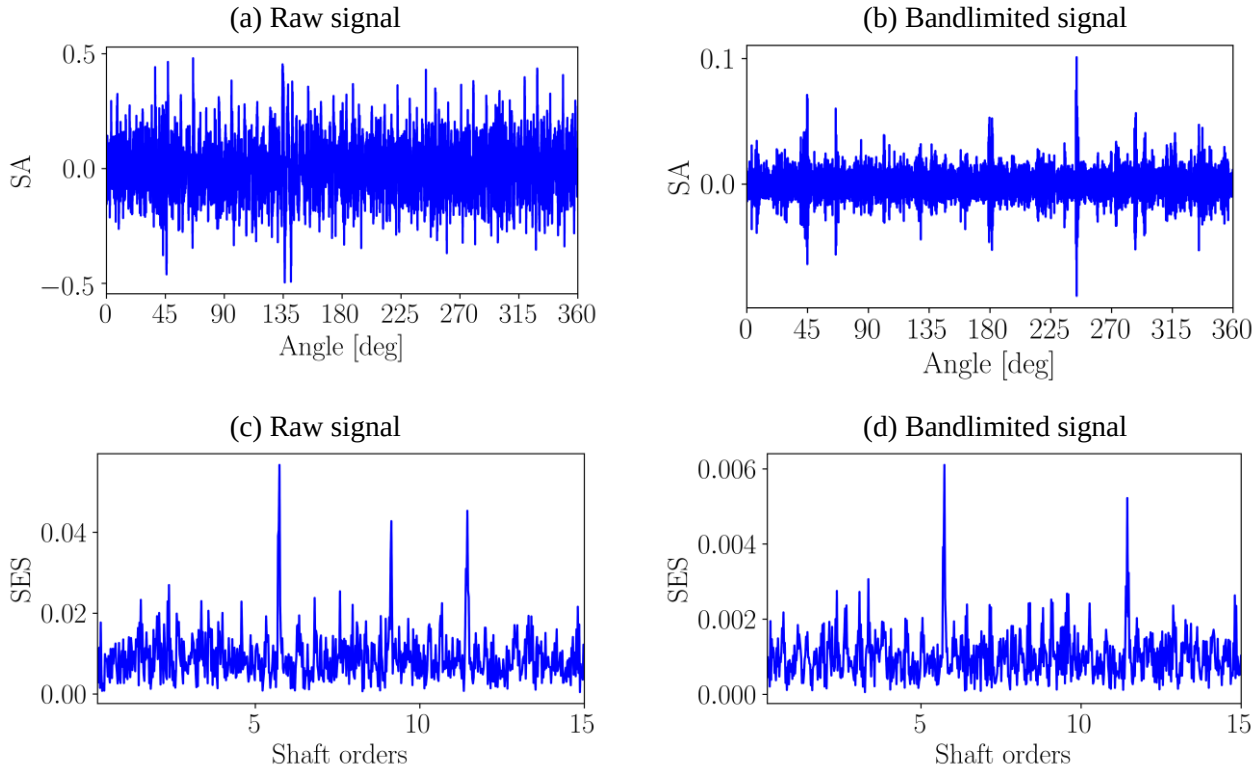

Figure 10: The Synchronous Average (SA) and the Squared Envelope Spectrum (SES of the raw and the bandlimited signals are shown as obtained with the Fast Kurtogram (FK). The damaged gear tooth is located at approximately 135 degrees in the SA plots.

The SES of the raw and the bandlimited signals are also investigated in Figure 10. Three peaks are observed in the SES of the raw signal; the components at 5.72 and 11.44 shaft orders are attributed to the

transients in the signal and the component at 9.12 shaft orders is attributed to the alternator's shaft being slightly unbalanced which resulted in periodical excitations. After, the filtering process, only the transient at 5.72 shaft orders and its harmonics are retained. Hence, it is evident from the results that the kurtogram fails to recognise the important frequency band for diagnosing the gear.

4.3 Application of the proposed method

The proposed method is applied on the same signal as investigated in the previous section. The gear and the pinion are monitored and therefore the decomposition is performed for $\{\alpha_f\}=\{1.0, 2.0, 3.0\}$ shaft orders (denoted $\alpha=1$) and $\{\alpha_f\} = \{1.85, 3.7, 5.55\}$ shaft orders (denoted $\alpha=1.85$), respectively. The feature plane is shown in Figure 11 for the two monitored components, where it can be seen that the feature planes are dependent on the cyclic order of interest, however, the identified frequency bands may not necessarily be completely separated. It is completely reasonable that the same cyclic order band is optimal for different mechanical components and therefore care should be taken to interpret the statistics (e.g. kurtosis) of the bandlimited signals.

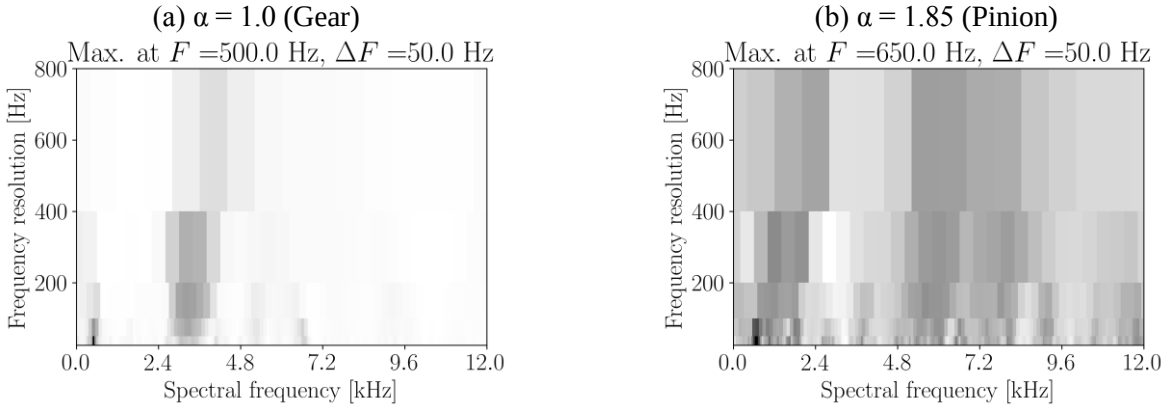

Figure 11: The feature plane obtained with the proposed method. The feature plane of the gear is shown in (a) and the feature plane of the pinion is shown in (b).

The SA in Figure 12 do not clearly reveal damage on either the gear or pinion with only small peaks seen at 135deg for the gear. This is attributed to the fact that the damage is still small and that helical gears are used with large contact ratios. Hence, the synchronous average is ineffective for detecting the incipient gear damage.

The SES of the raw and bandlimited signals in Figure 13 perform significantly better than the SA for the gear and the pinion. It is possible to see that there is a clear 1.0 shaft order component, which is attributed to the damaged gear. In contrast, the SES of the healthy pinion does not contain any dominant components at 1.85 shaft orders, which is indicative that the pinion is healthy. Hence, it is possible to use the proposed method and the SES to detect the incipient gear damage in the presence of dominant frequency components and time-varying operating conditions.

5 Conclusions

In this paper, a new method is investigated for identifying frequency bands that are rich with diagnostic information. The method uses the spectral coherence and a very carefully designed feature to allow specific frequency bands to be detected which can be analysed using the squared envelope spectrum and the synchronous average.

The method is evaluated on two datasets; the first one is a numerical gearbox dataset that simulates bearing damage and gear damage under time-varying speed conditions. The results indicate that it is possible to identify the appropriate frequency band to identify the cyclic components of interest, while the fast kurtogram only identifies the frequency band with the most impulsiveness. Similar results are obtained on the experimental dataset where incipient damage was present on the gear of a helical gearbox. The fast

kurtogram maximised on frequency bands with strong impulsive content, with the incipient gear damage only detected by using the proposed method. It was also found that the synchronous average is not very effective for incipient gear damage detection and the squared envelope spectrum performs significantly better.

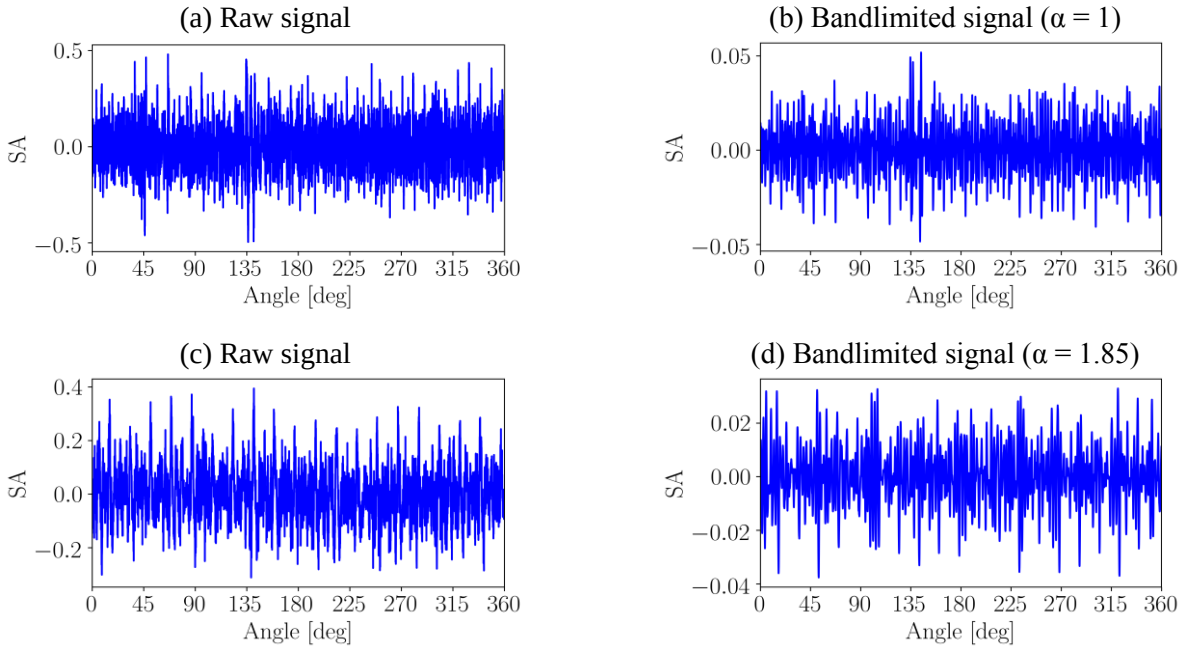

Figure 12: The Synchronous Averages (SA) of the raw and the bandlimited signals, obtained with the proposed method, are shown. The result for the gear is shown in (a) and (b), while the result of the pinion is shown in (c) and (d).

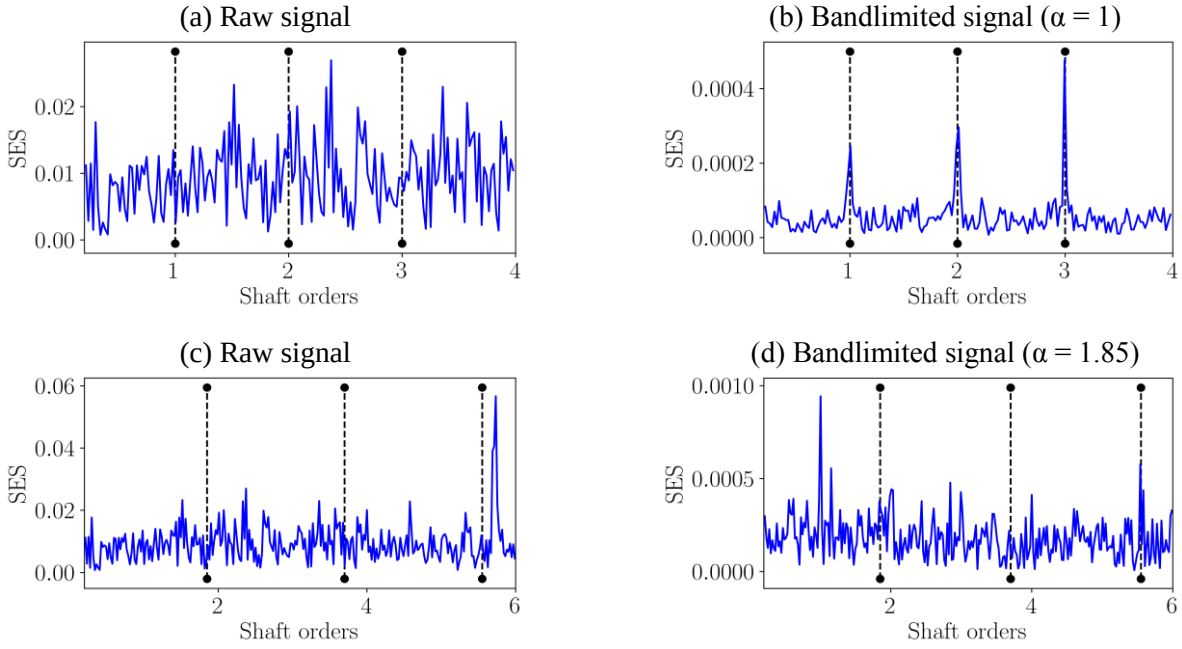

Figure 13: The Squared Envelope Spectra (SES) of the raw and the bandlimited signals, obtained with the proposed method are shown. In (a) and (b) the results for the gear are shown, while the results for the pinion are shown in (c) and (d).

In future investigations, the method will be compared to the more recent developments in the informative frequency band identification field (e.g. infogram) and the suitability of this method for fault diagnosis under time-varying operating conditions will be investigated on more datasets. It is also suggested that the spectral

coherence needs to be estimated with the fast or faster spectral correlation instead of the Welch estimator used in this work. This would improve the computational efficiency of the proposed method.

Acknowledgments

The authors gratefully acknowledge the support that was received from the Eskom Power Plant Engineering Institute (EPPEI) in the execution of the research.

References

[1] Abboud, D. & Antoni, J., 2017. Order-frequency analysis of machine signals. Mechanical Systems and Signal Processing, 87, pp.229–258.

[2] Abboud, D., Baudin, S., Antoni, J., Rémond, D., Eltabach, M. and Sauvage, O., 2016. The spectral analysis of cyclo-non-stationary signals. Mechanical Systems and Signal Processing, 75, pp.280-300.

[3] Abboud, D., Antoni, J., Sieg-Zieba, S. and Eltabach, M., 2017. Envelope analysis of rotating machine vibrations in variable speed conditions: A comprehensive treatment. Mechanical Systems and Signal Processing, 84, pp.200-226.

[4] Schmidt, S., Heyns, P.S. & Gryllias, K.C., 2019. A pre-processing methodology to enhance novel information for rotating machine diagnostics. Mechanical Systems and Signal Processing, 124, pp.541-561.

[5] Antoni, J. & Randall, R.B., 2006. The spectral kurtosis: Application to the vibratory surveillance and diagnostics of rotating machines. Mechanical Systems and Signal Processing, 20(2), pp.308–331.

[6] Antoni, J., 2007. Fast computation of the kurtogram for the detection of transient faults. Mechanical Systems and Signal Processing, 21(1), pp.108–124.

[7] Barszcz, T. & Randall, R.B., 2009. Application of spectral kurtosis for detection of a tooth crack in the planetary gear of a wind turbine. Mechanical Systems and Signal Processing, 23(4), pp.1352–1365.

[8] Antoni, J., 2016. The infogram: Entropic evidence of the signature of repetitive transients. Mechanical Systems and Signal Processing, 74, pp.73–94.

[9] Mauricio A, Qi J, & Gryllias K. 2018. Vibration-based condition monitoring of wind turbine gearboxes based on cyclostationary analysis. ASME. Journal of Engineering Gas Turbines Power.

[10] Stander, C.J., Heyns, P.S. & Schoombie, W., 2002. Using vibration monitoring for local fault detection on gears operating under fluctuating load conditions. Mechanical Systems and Signal Processing, 16(6), pp.1005–1024.

[11] Antoni, J., Xin, G. & Hamzaoui, N., 2017. Fast computation of the spectral correlation. Mechanical Systems and Signal Processing, 92, pp.248–277.

[12] Borghesani, P. & Antoni, J., 2018. A faster algorithm for the calculation of the fast spectral correlation. Mechanical Systems and Signal Processing, 111, pp.113–118.

[13] Schmidt, S., Heyns, P.S. & De Villiers, J.P., 2018. A tacholess order tracking methodology based on a probabilistic approach to incorporate angular acceleration information into the maxima tracking process. Mechanical Systems and Signal Processing, 100, pp.630-646.